A Geospatial Framework for Landslide Risk Assessment of Road Infrastructure at a Regional Level in Greece

Zoe Misiri , Alkistis Antonopoulou , Nikolaos Depountis * , Panagiotis Ioannidis , Andreas Kazantzidis

Posted Date: 23 April 2026

doi: 10.20944/preprints202604.1639.v1

Keywords: Landslide Susceptibility Index; Frequency Ratio; regional scale; risk assessment; road network

 doi:10.20944/preprints202604.1639.v1

Article

A Geospatial Framework for Landslide Risk Assessment of Road Infrastructure at a Regional Level in Greece

Zoe Misiri [1], Alkistis Antonopoulou [1], Nikolaos Depountis [1,*], Panagiotis Ioannidis [2] and Andreas Kazantzidis [2]

[1] University of Patras, Department of Geology, 265 04 Patras, Greece
[2] University of Patras, Department of Physics, 265 04 Patras, Greece
* Correspondence: ndepountis@upatras.gr; Tel.: +30-2610997715

Abstract

This study presents a comprehensive geospatial framework for landslide risk assessment across the 4,523 km road network of the Region of Epirus in Greece. Utilizing a field-verified inventory of 295 active landslides, the research evaluates five key predisposing factors—lithology, slope inclination, elevation, land use, and cumulative annual precipitation—using the bivariate Frequency Ratio (FR) statistical model. Among six tested scenarios, the most robust model integrated all factors, achieving high predictive accuracy by classifying nearly 80% of the study area within Moderate to Very High susceptibility zones. The resulting Landslide Susceptibility Index (LSI) was converted into a Landslide Hazard Index (LHI) and integrated with a weighted Road Vulnerability Map, which categorized road sectors based on functional importance and traffic volume. The final Landslide Risk Map indicates that the most critical risk zones are clustered along major transportation corridors that traverse geologically weak formations, moderate to high precipitation areas and steep mountainous sectors. This quantitative approach provides a vital decision-support tool for regional authorities, enabling the prioritization of geotechnical monitoring and the strategic allocation of resources for infrastructure stabilization. The methodology offers a replicable workflow for enhancing the resilience of transportation networks in landslide-prone Mediterranean regions facing evolving climatic threats.

Keywords: Landslide Susceptibility Index; Frequency Ratio; regional scale; risk assessment; road network

1. Introduction

Natural hazard management relies heavily on hazard assessment, which aims to determine both the spatial and temporal probability of catastrophic events [1]. This predictive capability is essential for evaluating potential socio-economic impacts and enabling the design of resilient infrastructure and the implementation of proactive mitigation measures [2].

Among the most frequent and devastating natural hazards globally, landslides pose significant risks to the environment, economic development, and human safety, often resulting in substantial damage to residential property and critical infrastructure [3–5]. Driven by complex geological settings and increasing urban development and infrastructure expansion, landslides are becoming more hazardous due to growing exposure and vulnerability [6]. In addition, the increasing occurrence of extreme climatic events associated with climate change is expected to further intensify landslide frequency and magnitude [7,8], presenting an escalating threat to human activities and economic assets.

Landslides are widely spatially distributed across Europe, with their occurrence influenced by various topographic and geo-environmental factors, often dictated by each country's unique geological, geomorphological, and environmental conditions. In Greece, landslides are

 doi:10.20944/preprints202604.1639.v1

predominantly associated with mountainous and hilly areas, road network, coastal regions, and riverbanks. Specific site conditions, such as lithology, slope inclination, rainfall accumulation, hydrology, and active tectonics, are among the most significant factors in determining landslide susceptibility, hazard and risk status [9].

While the aforementioned conditions predispose areas to landslides, external triggers serve as the immediate causes of landslide activation. In Greece, the most frequent triggers are related to increasingly extreme weather events, such as intense or prolonged rainfalls, often associated with floods [10,11]. Other natural triggers include earthquakes, as well as natural erosion along coastlines and riverbanks [12,13]. Human activities also significantly contribute to landslide initiation, as any interference with a slope influences its equilibrium. Since it is anticipated that landslides triggered by extreme rainfall events will increase in the future due to climate change, there is an urgent need for landslide recording, enhanced early warning and monitoring, risk assessment, and predictive capabilities in affected areas to protect communities, infrastructures, and preserve human activities [14–16].

To address this, landslide inventories and susceptibility maps have been developed in many countries worldwide, including at small-scale European and global levels [17,18]. A European Landslide Susceptibility Map is available through the European Soil Data Centre (ESDAC) [19–21]. Furthermore, the Global Landslide Catalog (GLC), published in 2019 and incorporating NASA's landslide datasets along with additional scientific reports, is publicly available online [22,23] however, it requires continuous updating and integration with newly available landslide datasets.

A landslide inventory is defined as a systematic record of the location, classification, volume, activity status, and date of occurrence of landslides [17,24]. In Greece, a national landslide inventory has been compiled and published by the Hellenic Survey of Geology and Mineral Exploration (HSGME) [25]. In addition, a regional Landslide Inventory Platform, named He.L.P. (Hellenic Landslide Platform), is currently under development by the Laboratory of Engineering Geology at the University of Patras, Greece [26].

He.L.P. is a web-based GIS platform that provides detailed information on landslide phenomena recorded over time within Western Greece, as defined by the administrative regions of Western Greece, Epirus, and the Ionian Islands. The platform integrates spatial and descriptive data, supporting landslide documentation, monitoring, and hazard assessment at the regional scale.

Recent advancements in computational tools and Geographic Information Systems (GIS) have significantly improved the development of susceptibility models that analyze the interaction between environmental predisposing factors and triggering mechanisms [1,18,27]. These models provide a spatial understanding of where landslides are more likely to occur, which forms the basis for landslide hazard assessment. However, hazard alone does not fully capture the potential consequences of landslides [28]. Therefore, it is important to distinguish between landslide hazard and risk.

Landslide hazard refers to the probability of occurrence of a landslide event of a given magnitude, within a specific area and a predetermined period of time [1,24,27,29], whereas landslide risk considers the potential impacts on exposed elements such as population, infrastructure, and economic activities [24,29]. In this sense, GIS-based hazard assessments serve as a critical input for risk analysis, as they help identify areas where the likelihood of landslides intersects with vulnerable assets.

Any susceptibility or risk analysis requires a comprehensive understanding of both the physical process and the resulting socioeconomic impacts [30,31]. To evaluate these components, researchers utilize two primary modeling categories: qualitative and quantitative [27,30,31]. Qualitative models are primarily heuristic, relying on expert judgment, while quantitative models provide a numerical estimate of occurrence. The current study applies to a quantitative method, the bivariate Frequency Ratio (FR) model [32,33], which is widely recognized as an effective statistical method for susceptibility mapping at the regional scale [27,28,30]. The FR model was selected due to its transparency and ability to quantify the spatial relationship between landslide distribution and

 doi:10.20944/preprints202604.1639.v1

individual conditioning factors without the interpretability issues often associated with complex algorithms [18,34].

As a study area for applying the Frequency Ratio (FR) quantitative method for landslide susceptibility assessment, the region of Epirus was selected. This region is highly prone to landslides due to its rugged terrain, significant elevation differences, and complex geological structure, which is largely dominated by Flysch formations [9,35]. The analysis, based on a detailed inventory of 295 active events [25,26], incorporates five decisive parameters: lithology and slope inclination as fundamental intrinsic factors [36,37], alongside elevation, land use, and cumulative annual precipitation [29,38,39].

Special emphasis was placed on cumulative annual precipitation, which acts as a dynamic trigger and a primary conditioning agent in Western Greece [10,11,15,29]. Rainfall data were derived from the ERA5-Land reanalysis dataset [39,40], which provides high-resolution meteorological variables (~9 km) by evolving the Copernicus Climate Change Service (C3S) models. The use of reanalysis data is particularly valuable in rugged terrains like Epirus, where ground-based monitoring networks may be sparse or irregularly spaced [40,41], ensuring the physical validity of the spatial rainfall distribution and overcoming the limitations of traditional interpolation methods [11,12,41].

One of the objectives of this study is to develop a GIS-based landslide susceptibility assessment for the region of Epirus using the bivariate Frequency Ratio (FR) method. The resulting susceptibility map is subsequently integrated with the regional road network (4,523 km) to identify and classify road segments according to their relative exposure to landslide-prone areas (low, medium, and high). By linking susceptibility patterns with critical transportation infrastructure, the study aims to provide an integrated landslide risk assessment of road infrastructure at a regional level, a spatial decision-support tool that can assist regional authorities in prioritizing monitoring, mitigation measures, and infrastructure planning in one of the most landslide-prone regions of the Mediterranean.

2. Study Area and Research Material

2.1. Landslide Inventory of the Study Area

The development of a comprehensive landslide inventory is a fundamental requirement for any susceptibility analysis, as it provides the essential reference data for the application of statistical models. In this study, the landslide inventory of the study area was designed using the He.L.P. database [26]. The associated platform draws all its data from this geographic database, and in this way, the end user has access to satellite imagery of the area along with information such as the inventory code, geographical location based on the administrative divisions of Greece, coordinates projected at the Hellenic Geodetic Reference System 1987 (GGRS87), type of landslide, and a Landslide Inventory Form (LIF) available as a PDF sheet.

The selected study area, Region of Epirus, is characterized by a complex geological structure resulting from Alpine orogenic tectonics. The prevailing geological formations consist of Alpine bedrock (flysch and limestones), as well as post-Alpine Neogene and Quaternary formations [35]. These formations are strongly tectonized and are often covered by a weathered zone of varying thickness; consequently, most landslides occur within these formations. Geomorphology is steep and mountainous and is significantly affected by prolonged rainfall events. Slope inclination, elevation, cumulative rainfall, land use, and lithology are the main predisposing factors controlling the frequency and spatial distribution of landslide occurrences in the Region of Epirus and were therefore investigated in this study.

A total of 295 landslides (Figure 1) were identified in the Region of Epirus and integrated into the database and the platform. It should be noted that the actual number of landslides in the area is higher; however, for the purposes of this analysis, only those landslides that were verified in the field by the research team were considered.

 doi:10.20944/preprints202604.1639.v1

According to most well-known landslide classification systems [36,37], the recorded events display a wide range of movement types. Earth and rock flows constitute the most frequent category, accounting for 39% of the total inventory, followed by complex landslides (21%) and rotational slides (15%).

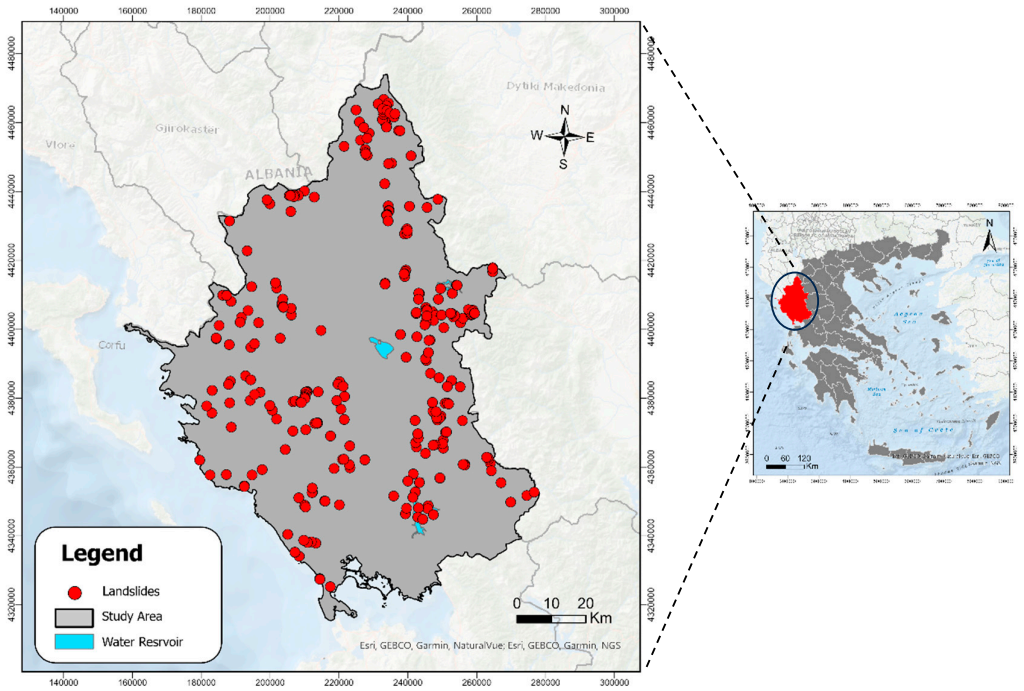

Figure 1. Landslide Inventory of the Region of Epirus, Greece.

2.2. Lithology

For susceptibility assessment, the geological background constitutes a fundamental factor, depending on the scale applied in the model. In the present study, a geological/lithological map of the study area at a scale of 1:50,000 was used as the primary baseline dataset (Figure 2). This map was compiled by the Laboratory of Engineering Geology at the University of Patras using Geographic Information Systems (GIS) techniques [26], based on the digitization of geological maps provided by the Hellenic Survey of Geology and Mineral Exploration (HSGME) [25].

A total of twelve (12) generalized geological formations are illustrated in Figure 2, corresponding to the lithological classes adopted for the purposes of the present study (Table 1).

Table 1. Lithological description of the geological formations of the study area.

Class	Geological Formations	Lithological Description
1	Allouvial deposits (al)	Unconsolidated silts and sands with low shear strength. Highly sensitive to water saturation and riverbank erosion.
2	Scree (SC)	Loose, coarse rock fragments with no cohesion. Highly unstable on steep slopes and sensitive to intense rainfall.
3	Neogene (N-m)	Marls, sandstones, and conglomerates.
4	Flysch Gavrovo zone (fl-G)	Rhythmic sequences of sandstones and shales. Highly tectonized with low shear strength
5	Flysch Ionian zone (fl-I)	Strongly folded and sheared sequences of sandstones and siltstones.
6	Flysch Pindos zone (fl-P)	Densely folded and highly fractured turbidites. Characterized by high tectonic deformation
7	Limestones Gavrovo zone (lm-G)	Massive to thickly bedded neritic limestones.

 doi:10.20944/preprints202604.1639.v1

8	Limestones Ionian zone (lm-I)	Well-bedded pelagic limestones with frequent chert nodules.
9	Limestones Pindos zone (lm-P)	Thin-bedded pelagic limestones with frequent intercalations of platy cherts. Highly folded and fractured.
10	Limestones Sub-pelagonian zone (lm-Y)	Massive to medium-bedded neritic limestones, often associated with tectonic contacts.
11	Evaporites (G)	Highly soluble sulfate formations.
12	Ophiolites (of)	Heterogeneous sequence of basic and ultrabasic rocks. Highly serpentinized and sheared, behaving as a soil-like mass in weathered zones with extreme susceptibility to complex landslides

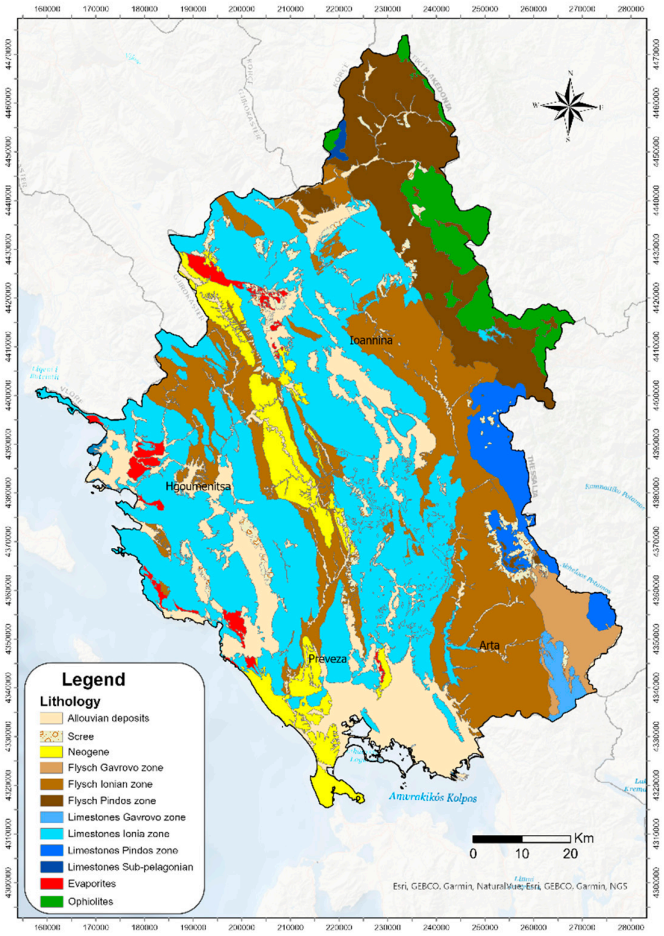

Figure 2. Generalized Geological Map of the Region of Epirus, Greece.

2.3. Slope Inclination

The slope factor refers directly to surface inclination and was calculated using a high-resolution (5 × 5 m) Digital Surface Model (DSM) provided by the Greek Cadastral for the study area (Figure 3).

The slope classes selected for the construction of the map presented in Figure 3 were defined using a constant interval of 15°, specifically: 0°–15°, 15°–30°, 30°–45°, and >45°. The selection of these intervals was based on: (a) the calculated standard deviation and the maximum slope value, (b) the slope gradient limits proposed by the Hellenic Technical Specification ELOT TP 1501-02-02-01, and (c) the fact that slope values follow an approximately normal distribution across the four resulting classes [42]. This classification approach is consistent with established cartographic methods for landform analysis and landslide susceptibility modeling [18,42].

 doi:10.20944/preprints202604.1639.v1

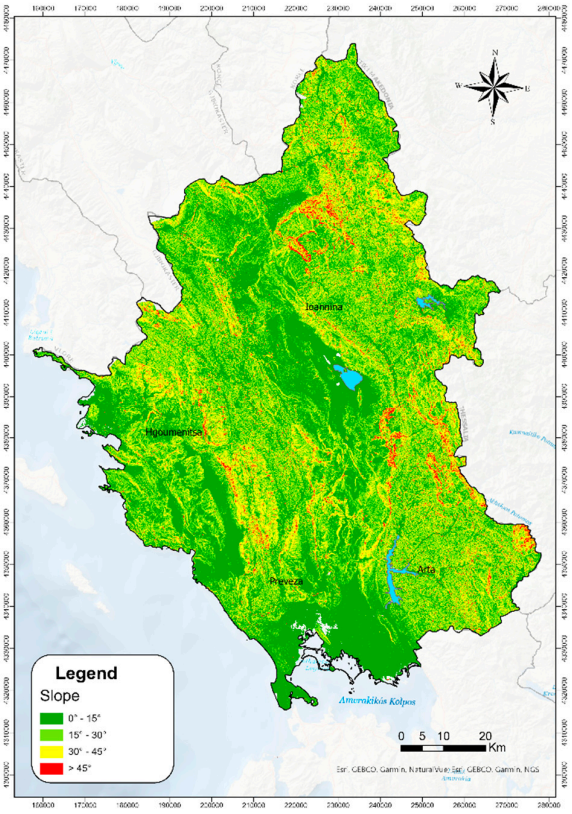

Figure 3. Slope Inclination Map of the of the Region of Epirus, Greece.

2.4. Elevation

Elevation data were derived from the high-resolution (5 × 5 m) Digital Surface Model (DSM) provided by the Greek Cadastral. Within the study area, the maximum observed elevation reaches 2,629 m, while the mean elevation is 692.15 m.

For the purposes of susceptibility analysis, it was necessary to establish elevation classes covering the entire study area. According to the Hellenic Statistical Authority, Greece is divided into the following altitudinal zones: Lowland (0–400 m), Semi-mountainous (400–600 m), and Mountainous (>600 m). However, this classification was considered too coarse for the objectives of the present study. Consequently, the categorization adopted by the Civil Protection Directorate and the Hellenic National Meteorological Service (HNMS) for issuing Severe Weather Warnings was applied (Table 2), in accordance with the HNMS altitudinal zone definition [43].

Table 2. Elevation Classes (HNMS Standards).

Class	Morphological Zone	Elevation Range (m)
1	Lowland	0-300
2	Hilly	301-600
3	Semi-mountainous	601-900
4	Mountainous	>900

In the Digital Elevation Map of the Region of Epirus, the distinction between high- and low-altitude areas is clearly illustrated through color gradation. The highest elevations are observed along the Pindos mountain range, whereas the lowest altitudes are primarily located in the western and southern parts of the study area (Figure 4).

 doi:10.20944/preprints202604.1639.v1

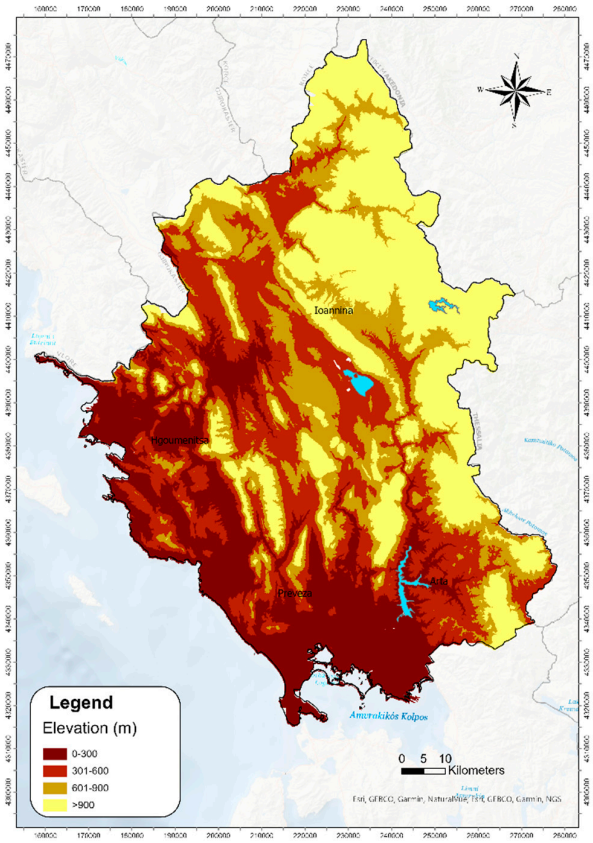

Figure 4. Digital Elevation Map (DEM) of the region of Epirus.

2.5. Land Use

Land use classification was performed based on the CORINE Land Cover 2018 (CLC 2018) inventory, which forms part of the pan-European land cover database [38]. This program provides standardized land use and land cover mapping for several European countries, including Greece, at a spatial scale of 1:100,000.

Within the study area, a total of six (6) aggregated land cover categories were identified as presented in Figure 5 and Table 3. The integration of these categories into the susceptibility model allows for the assessment of how different vegetation types and human activities affect the spatial distribution of landslide events [18,29].

Table 3. Land Use Categories with description.

Class	Land Use Category	Description
1	Residential areas and Infrastructure	Continuous and discontinuous urban fabric, industrial units, and the transport network (roads and railways).
2	Agricultural Areas	Arable land, permanent crops (orchards, olive groves), and heterogeneous agricultural zones.
3	Forests	Areas dominated by tree vegetation, including broad-leaved, coniferous, and mixed forest formations.
4	Shrub & Herbaceous	Sclerophyllous vegetation, moors, heathlands, and natural grasslands.
5	Bare Land	Areas with little or no vegetation, including bare rocks, burnt areas, and sparsely vegetated slopes.
6	Water Bodies	Inland waters such as river courses, natural or artificial lakes

 doi:10.20944/preprints202604.1639.v1

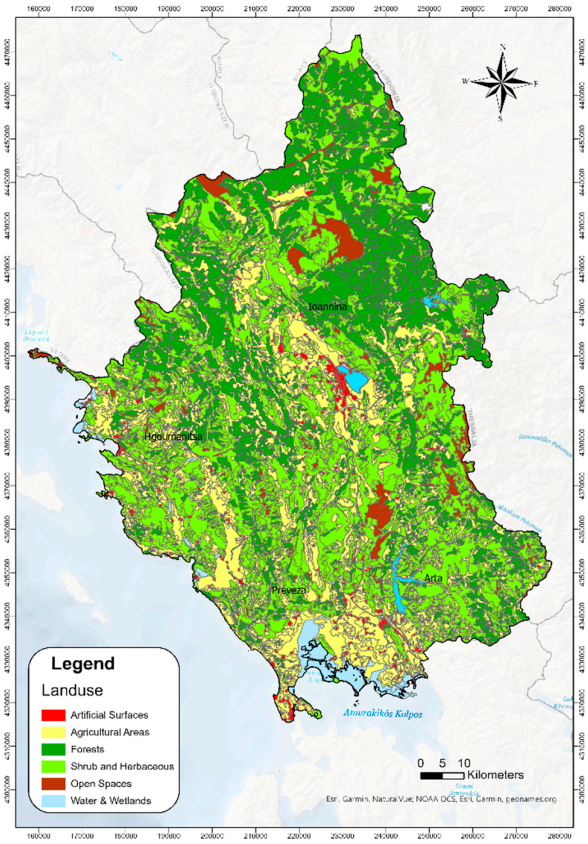

Figure 5. Land Use Map of the Region of Epirus.

2.6. Cumulative Annual Precipitation

Hourly reanalysis data for the period from 01-01-1980 to 01-06-2024 were retrieved from the ERA5-Land dataset [39,40]. The extraction was performed automatically using the Copernicus Climate Data Store (CDS) API [39] through an official Python script. The data were downloaded in NetCDF format for a spatial domain covering latitudes 38.6°–40.7° N and longitudes 19.5°–21.9° E, encompassing the study area in Western Greece.

To ensure consistent temporal aggregation and precise location-specific outputs, the Inverse Distance Weighting (IDW) interpolation method was applied [41]. The hourly dataset was resampled into daily, monthly, and annual intervals. Precipitation totals were accumulated and averaged to represent mean climatological conditions. Each resampling operation generated a new NetCDF file, ensuring that all vital metadata were preserved throughout the process.

The final geospatial analysis was conducted within a GIS environment, leading to the generation of the cumulative annual precipitation map (Figure 6). The spatial data were classified into four (4) distinct categories using the Equal Interval classification method [42]. This approach divides the range of attribute values into equal-sized sub-ranges, providing a clear and objective representation of rainfall intensity magnitude and its spatial distribution across the Epirus region.

 doi:10.20944/preprints202604.1639.v1

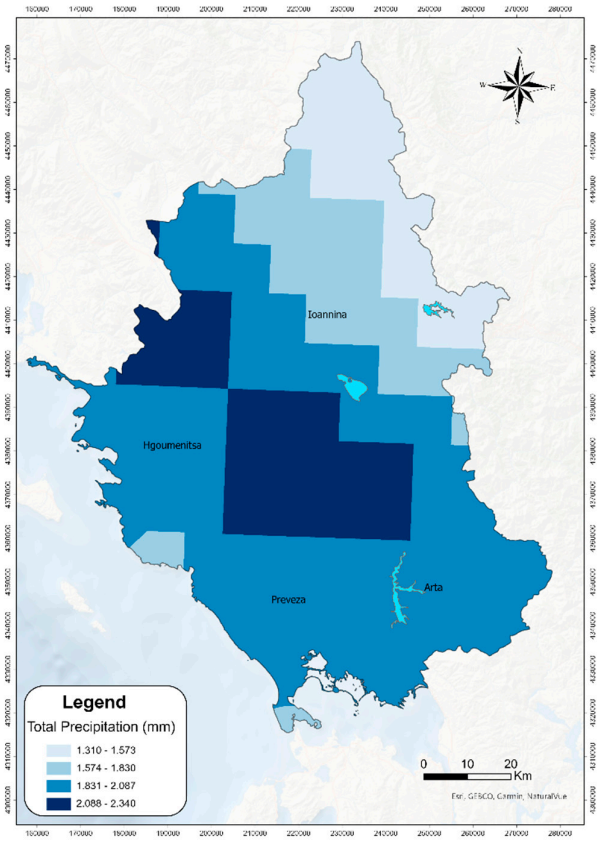

Figure 6. Cumulative Annual Precipitation Map of the Region of Epirus.

3. Methods and Materials

3.1. Methodological Framework

The methodology implemented in this research initially involves the integration of all landslides predisposing factors (lithology, slope inclination, elevation, land use, and cumulative precipitation), in the form of raster maps as previously described, with the use of Geographic Information System (GIS) [17,18].

To quantify the relationship between these factors and the spatial distribution of landslides, a bivariate statistical approach, namely, the Frequency Ratio (FR) method is adopted [33,34]. The spatial distribution of recorded landslides is used as the dependent variable in the FR model. This enabled the correlation of historical landslide occurrences with the five predisposing factors, thereby facilitating the quantification of landslide susceptibility across the regional territory [18,29].

The final degree of landslide susceptibility is determined using the Landslide Susceptibility Index (LSI), a dimensionless quantitative indicator that expresses the relative likelihood of landslide occurrence in a given area based on predisposing environmental factors. The LSI represents the relative spatial probability of landslide occurrence, derived from the weighted combination of conditioning factors and historical landslide data, without considering temporal probability or potential consequences (damage or losses) [18,21].

Due to limitations in estimating temporal probability, a conservative assumption is adopted in this study, whereby the probability of occurrence is considered equal to one (P = 1). Under this assumption, the Landslide Susceptibility Index (LSI) is considered equivalent to the Landslide Hazard Index (LHI).

In this context, the Element at Risk is specifically defined as the road network of Epirus, which constitutes the most critical infrastructure exposed to potential slope failures [9,14]. To assess the impact, the Vulnerability of the network is quantified based on its traffic load, reflecting the socio-

 doi:10.20944/preprints202604.1639.v1

economic importance and the volume of daily commuters exposed. This vulnerability is assigned a discrete three-class ranking system (1–3), where Class 1 represents local or secondary roads with low traffic, Class 2 includes Provincial roads with moderate traffic, and Class 3 corresponds to major National roads, which are characterized by heavy traffic load.

The final stage of the methodology involves the quantification of landslide risk by integrating the three primary components: Hazard, Exposure, and Vulnerability [24,30,31]. In this research, the landslide risk assessment is executed through a geospatial multiplication process in a GIS environment, following the comprehensive risk equation (Eq. 1):

$$\text{Risk} = \text{Hazard X Vulnerability X Element at Risk} \quad (1)$$

This process results in the development of a Landslide Risk Map for regional road infrastructure, with the methodological framework presented in Figure 7.

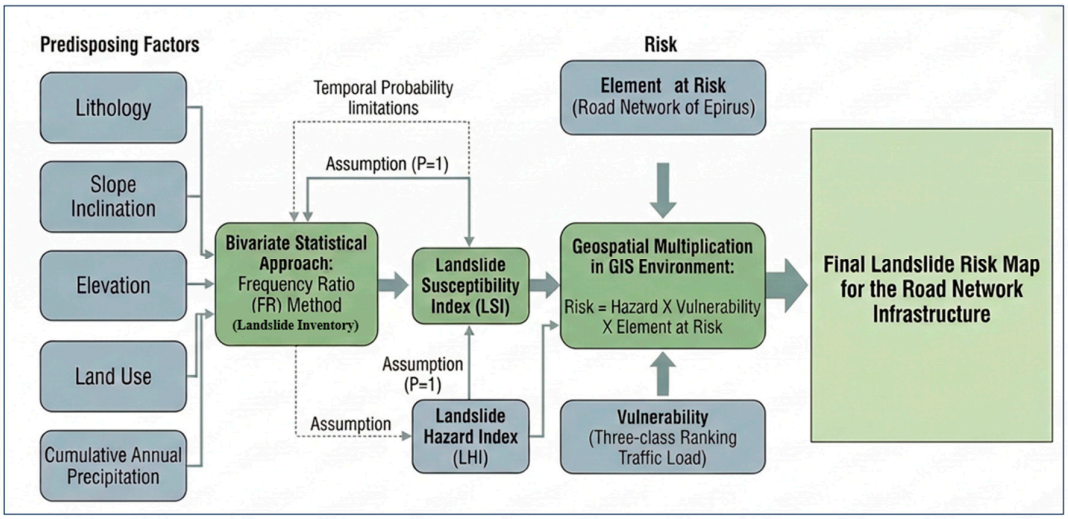

Figure 7. Methodological Framework for Landslide Risk Assessment of a Road Network.

3.2. Frequency Ratio and Landslide Susceptibility Index

The Frequency Ratio (FR) method used to analyze the relationship between the spatial distribution of landslides and their predisposing factors within a specific area and calculate the number of landslides occurring within each class of every factor. The frequency ratio for each class is then obtained by dividing the landslide occurrence ratio by the corresponding area ratio of that class [32,33].

An FR value greater than one (FR > 1) indicates a strong positive correlation between landslide occurrence and the specific factor class, whereas an FR value less than one (FR < 1) suggests a weak or negative correlation. The FR values for each class of the predisposing factors are calculated using Equation (2):

$$\text{FR} = \frac{\text{LF}}{\text{CA}} \quad (2)$$

where LF is the relative frequency of landslides (%) in a class of a factor, and CA is the percentage of the total area (%) covered by the same class.

Table 4 presents the FR values for each class of the predisposing factors, as calculated for the entire Region of Epirus.

 doi:10.20944/preprints202604.1639.v1

Table 4. Classification of predisposing factors and their statistical FR weights.

Factor	Class	Landslide frequency (Number)	(LF) %	Class area (CA) (km²)	(CA) %	FR
Lithology	Allouvian deposits (al)	22	7,46	1357,92	14,82	0,50
	Scree (SC)	10	3,39	223,86	2,44	1,39
	Neogene (N-m)	23	7,80	517,2365	5,65	1,38
	Flysch Gavrovo zone (fl-G)	9	3,05	209,70	2,29	1,33
	Flysch Ionian zone (fl-I)	106	35,93	1914,35	20,89	1,72
	Flysch Pindos zone (fl-P)	74	25,08	961,32	10,49	2,39
	Limestones Gavrovo zone (lm-G)	0	0,00	70,34	0,77	0,00
	Limestones Ionian zone (lm-I)	39	13,22	3129,20	34,15	0,39
	Limestones Pindos zone (lm-P)	4	1,36	289,38	3,16	0,43
	Limestones Sub-pelagonian zone (lm-Y)	1	0,34	16,25	0,18	1,91
	Evaporites (G)	1	0,34	119,60	1,31	0,26
	Ophiolites (of)	6	2,03	352,92	3,85	0,53
Elevation	0 - 300 m	41	13,90	2094,16	22,90	0,61
	300 - 600 m	66	22,37	2481,38	27,14	0,82
	600 - 900 m	104	35,25	1899,03	20,77	1,70
	> 900 m	84	28,47	2668,93	29,19	0,98
Slope Inclination	0° - 15°	60	20,34	3204,51	35,50	0,57
	15° - 30°	118	40,00	3644,41	40,37	0,99
	30° - 45°	85	28,81	1956,88	21,68	1,33
	> 45°	32	10,85	221,28	2,45	4,43
Land use	Residential areas and Infrastructure	13	4,41	178,68	1,94	2,27
	Agricultural Areas	67	22,71	2142,56	23,25	0,98
	Forests	80	27,12	2533,54	27,49	0,99
	Shrub & Herbaceous	125	42,37	3770,88	40,91	1,04
	Bare Land	10	3,39	358,34	3,89	0,87
	Water Bodies	0	0,00	232,90	2,53	0,00
Cumulative Annual Precipitacion (mm)	1310 – 1573 mm	74	25,08	1134,38	12,38	2,03
	1574 – 1830 mm	48	16,27	1435,50	15,66	1,04
	1831 – 2087 mm	106	35,93	4898,00	53,44	0,67
	2088 – 2340 mm	67	22,71	1697,87	18,52	1,23

The Landslide Susceptibility Index (LSI) is calculated using Equation (3):

$$LSI = \sum_{j=1}^{n} Wij \quad (3)$$

where *n* represents the total number of conditioning factors and Wij denotes the weight assigned to class *i* of factor *j* [32,33]. Higher LSI values correspond to greater landslide susceptibility.

 doi:10.20944/preprints202604.1639.v1

The Landslide Susceptibility Index (LSI) was computed by integrating the FR weights for each class of predisposing factors into the GIS, enabling the generation of multiple susceptibility maps under different factor-combination scenarios. [27,34]. Initially, all thematic layers were converted into a raster format with a uniform cell size to ensure spatial alignment. Each layer then underwent a reclassification process, where the raw data values were replaced by their respective Frequency Ratio (FR) weights derived from the statistical analysis. The final synthesis was performed using the Raster Calculator tool, which utilized Map Algebra to execute a pixel-by-pixel additive overlay. This tool processed the spatial distribution of all reclassified factors simultaneously, summing their individual weights for every grid cell across the study area. This systematic integration ensured high computational precision and allowed for the efficient generation of different susceptibility maps by adjusting the factor combinations for each evaluated scenario [21].

The baseline scenario (Scenario 1) includes all five predisposing factors. In the subsequent scenarios, one factor is systematically excluded at a time (Table 5) to evaluate its individual contribution to the overall reliability and predictive capability of the model. Using this approach, six different susceptibility maps were produced for the entire study area (Figure 8).

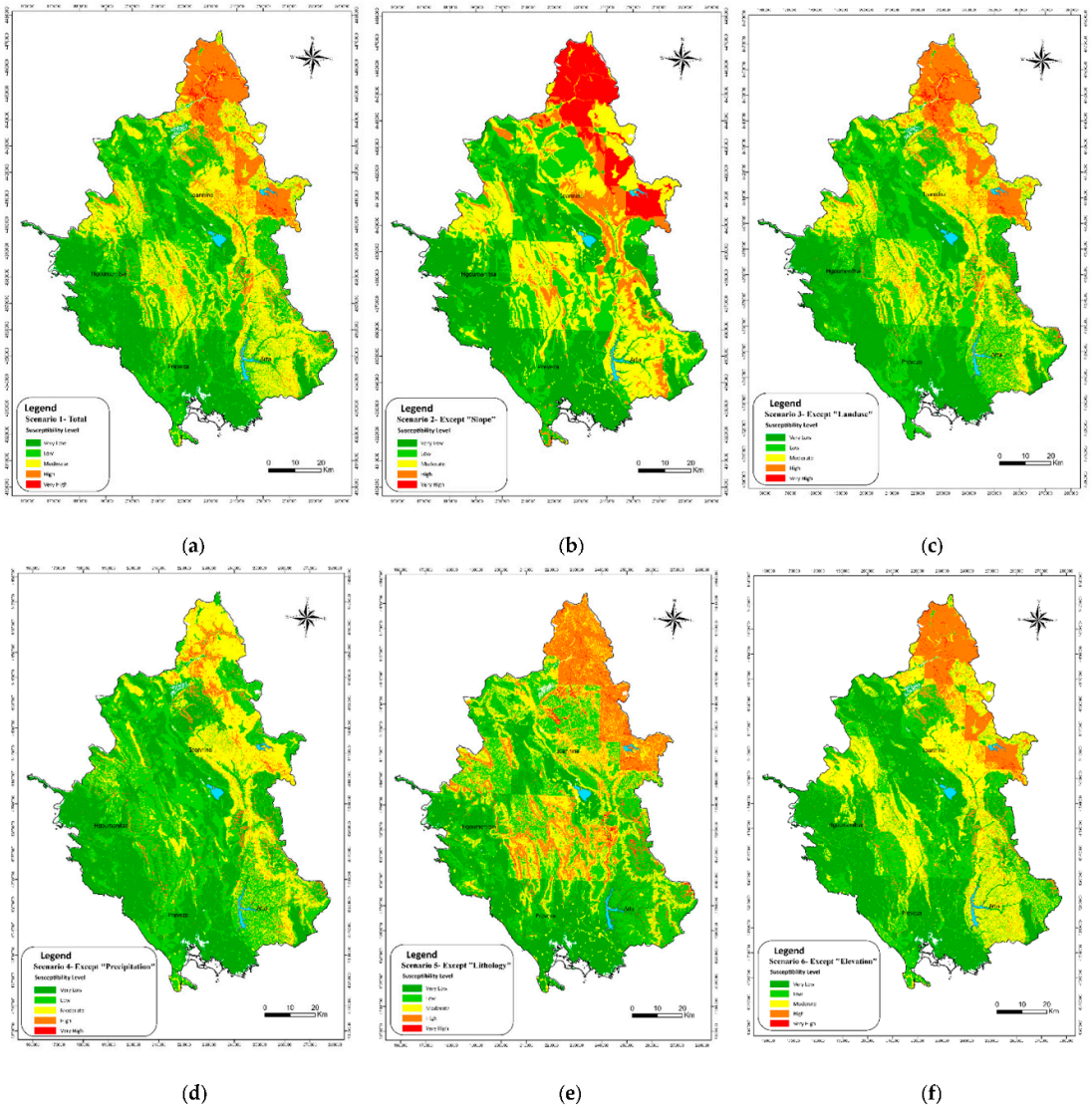

Figure 8. Landslide Susceptibility Index Maps of the Region of Epirus based on the six (6) scenarios presented in Table 1.

 doi:10.20944/preprints202604.1639.v1

Table 5. Landslide susceptibility scenarios considered in this study.

Class	Scenario n.1	Scenario n.2	Scenario n.3	Scenario n.4	Scenario n.5	Scenario n.6
Lithology	✓	✓	✓	✓	X	✓
Elevation	✓	✓	✓	✓	✓	X
Precipitation	✓	✓	✓	X	✓	✓
Land Use	✓	✓	X	✓	✓	✓
Slope	✓	X	✓	✓	✓	✓

In all the above maps, the spatial distribution of the Landslide Susceptibility Index (LSI) was classified into five categories: very low, low, moderate, high, and very high, using the Reclassify tool. The classification was based on the Natural Breaks statistical method, which optimizes the grouping of values by minimizing variance within each class while maximizing the differences between them.

The selection of the most appropriate model was based on identifying the scenario that concentrates the highest cumulative percentage of the study area within the three most important susceptibility classes (Moderate, High and Very High), as shown in Table 6. According to the data provided in Table 6 Scenario n.1 emerged as the optimal choice, as it achieves the highest predictive capability among the physically sound configurations, classifying 79,56% of the study area within the top susceptibility zones.

Table 6. Statistical Comparison of LSI Scenarios (n.1–n.6) by Percentage Area per Class.

Class	Scenario n.1	Scenario n.2	Scenario n.3	Scenario n.4	Scenario n.5	Scenario n.6	Susceptibility zone
1	5,42%	10,51%	6,10%	8,81%	6,44%	6,44%	Very Low
2	14,92%	12,88%	17,29%	26,10%	26,44%	15,25%	Low
3	40,68%	30,17%	39,66%	46,78%	28,14%	46,44%	Moderate
4	30,17%	20,68%	30,85%	12,20%	29,15%	25,76%	High
5	8,81%	25,76%	6,10%	6,10%	9,83%	6,10%	Very High

The selection of Scenario n.1 as the most reliable model is grounded in its comprehensive integration of the five primary predisposing factors, which include lithology, slope inclination, elevation, land use, and cumulative annual precipitation. As the baseline configuration, this scenario accounts for the multidimensional nature of landslide triggers in the Epirus Region, capturing the complex interactions between the geological environment and climatic drivers. Unlike Scenarios n.2 through n.6, which were utilized primarily as sensitivity tests by systematically excluding one variable at a time, Scenario n.1 provides a holistic representation of the physical environment. This inclusivity ensures that the model reflects the actual geo-environmental conditions where multiple factors often act in synergy to destabilize slopes.

The statistical validity of Scenario n.1 is further demonstrated by its superior predictive performance across the study area. In this research, the reliability of a susceptibility configuration was determined by its capacity to concentrate on the highest cumulative percentage of the region within the top three susceptibility classes: Moderate, High, and Very High. Scenario n.1 emerged as the optimal choice by classifying 79.56% of the total study area within these critical zones. Specifically, it accurately distributed the landscape into 40.68% Moderate, 30.17% High, and 8.81% Very High susceptibility zones. This distribution indicates a high degree of sensitivity in identifying hazardous areas compared to models that omitted key drivers like precipitation or lithology, which often resulted in a less precise spatial distribution of risk.

Finally, the robustness of Scenario n.1 is confirmed by the high Frequency Ratio (FR) values associated with its constituent factors, such as the significant weight of flysch formations and steep slope gradients. By incorporating all statistically relevant parameters, the model successfully captures the localized thresholds that lead to slope failure, such as the high susceptibility associated with

 doi:10.20944/preprints202604.1639.v1

cumulative annual precipitation exceeding 1,300 mm. Because Scenario n.1 achieved the highest predictive capability among all physically sound configurations, it was selected as the definitive foundation for the Landslide Hazard Index. This ensures that the subsequent risk assessment for the regional road infrastructure is based on the most statistically representative and scientifically rigorous susceptibility mapping available. Therefore, Scenario n.1 provides the most robust and representative basis for the final Landslide Susceptibility Map presented in Figure 8a for the Region of Epirus.

3.3. Landslide Hazard Index

Landslide hazard (LH) assessment constitutes a critical intermediate step in transitioning from statistical analysis to the risk evaluation of infrastructure [24,27]. Hazard is defined as the probability of a landslide occurring within a specific area over a given timeframe, resulting from the combination of spatial probability (LSI) and temporal probability (P) [1,27].

In the present study, the lack of sufficient historical data regarding the frequency and return periods of the 295 recorded landslide events made it challenging to accurately determine the temporal variable P. Consequently, a strategy was adopted in which spatial susceptibility was directly aligned with hazard, based on the assumption that geologically prone areas represent immediate sources of hazard.

By equating the temporal probability to unity (P = 1), LSI derived from the optimal Scenario n.1, was functionally transformed into Landslide Hazard Index (LHI) (Figure 9). This methodological assumption allowed spatial data to serve as the primary input for the risk assessment model, ensuring that the analysis focuses on the vulnerability and protection of the Epirus road network. In this way, the spatial distribution of susceptibility is converted into an operational prioritization tool, enabling the identification of road segments directly exposed to the threat of landslide events.

The Landslide Hazard Index (LHI) was classified using the Natural Breaks algorithm [44] into five categories: Very Low, Low, Moderate, High, and Very High

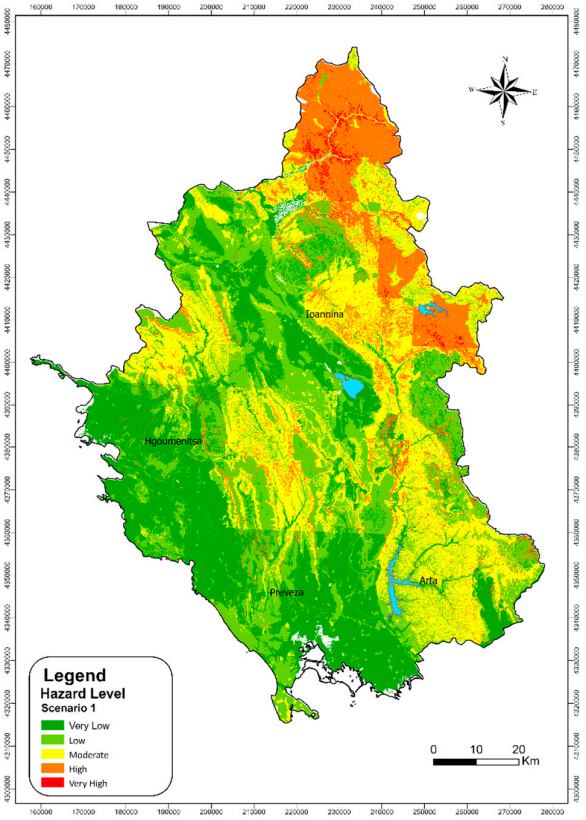

Figure 9. Landslide Hazard map of the Region of Epirus.

 doi:10.20944/preprints202604.1639.v1

3.4. Element at Risk and Vulnerability

The exposure analysis represents the phase of the risk assessment where the identified natural hazard intersects with human-made infrastructure [2,29]. In the context of this study, the Element at Risk is defined exclusively as the road infrastructure of the Region of Epirus. The road network is considered a critical asset, as any disruption caused by landslide activity entails significant socio-economic consequences, affecting regional connectivity and emergency response capabilities.

The quantitative basis of this analysis is the total road network of the study area, which spans a cumulative length of 4,523.54 km. This extensive dataset was integrated into a Geographic Information System (GIS) environment to facilitate spatial overlaying with the previously derived LHI and was classified based on its functional importance and hierarchy, distinguishing between national, provincial and other roads (Table 7).

Table 7. Classification of the road network in the Epirus Region.

Road Network Sector	Km
National Roads	1084,47
Provincial Roads	2729,85
Other Roads	709,22

This distinction is vital for the subsequent risk modeling, as the degree of exposure is not merely a matter of spatial presence but is also associated with the operational importance and traffic volume served by each road segment.

The vulnerability of the road network was quantitatively evaluated by assigning specific weighting values to each road sector, based on a combination of traffic volume and functional significance. The National Road Network received the highest weighting value of 3, as these corridors accommodate the primary traffic load and serve as the region's most critical transportation arteries. The Provincial Road Network was assigned a value of 2, reflecting its essential role in maintaining inter-municipal connectivity and supporting moderate traffic demands. Finally, all other roads were given a value of 1, representing sectors with lower traffic volumes and a more localized socio-economic impact. This weighted categorization was integrated into geospatial analysis to generate the final vulnerability road map of the Region of Epirus (Figure 10), which provides a spatial visualization of the infrastructure's susceptibility to disruption based on its relative importance to the regional network.

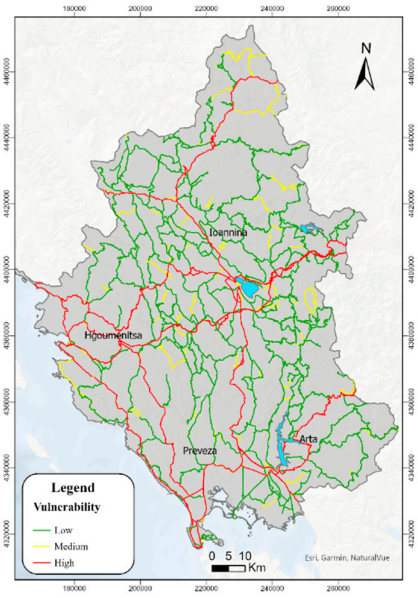

Figure 10. Vulnerability Road Map of the Region of Epirus.

 doi:10.20944/preprints202604.1639.v1

4. Results

4.1. Landslide Risk to the Road Network

The final phase of the geospatial framework involved the generation of the Landslide Risk Map for the road infrastructure of the Epirus Region. The risk assessment procedure was executed through a spatial synthesis of three primary components: the Landslide Susceptibility Index (LSI), the Landslide Hazard Index (LHI), and the weighted Road Vulnerability Map. By integrating these layers within a Geographic Information System (GIS) environment, the study transitioned from identifying potential slope instability to quantifying the specific threat posed to the 4,523 km regional transportation network. To ensure statistical consistency and practical utility for regional planning, the resulting risk values were classified into three qualitative categories—Low, Moderate, High—using the Natural Breaks optimization method [44].

The resulting Landslide Risk Map (Figure 11) reveals a high degree of spatial variability across the Epirus Region, reflecting the complex interplay between mountainous topography, flysch-dominated geology, and critical infrastructure. A primary observation from the map is the concentration of "High" risk sectors along the North-East axis of the region, where the National Road Network traverses steep terrain with flysch formations. Specifically, the analysis identifies significant risk clusters in the Pindus mountain range, where the combination of high functional vulnerability (National roads) and extreme landslide hazard creates high-priority zones for maintenance and mitigation.

Quantitatively, the results indicate that a significant portion of the Epirus road network is exposed to non-negligible risk levels. While the "Low" risk classes cover the flatter coastal and lowland areas, the "Moderate" and "High" risk classes are disproportionately represented in the semi-mountainous and mountainous interior. These moderate to high-risk sectors are of particular concern for regional authorities, as they represent areas where a landslide event would not only have a high probability of occurrence but would also result in maximum socio-economic disruption due to the strategic importance of the affected road segments. This map serves as a decision-support tool, allowing for the prioritization of site-specific geotechnical investigations and the strategic allocation of resources for slope stabilization works

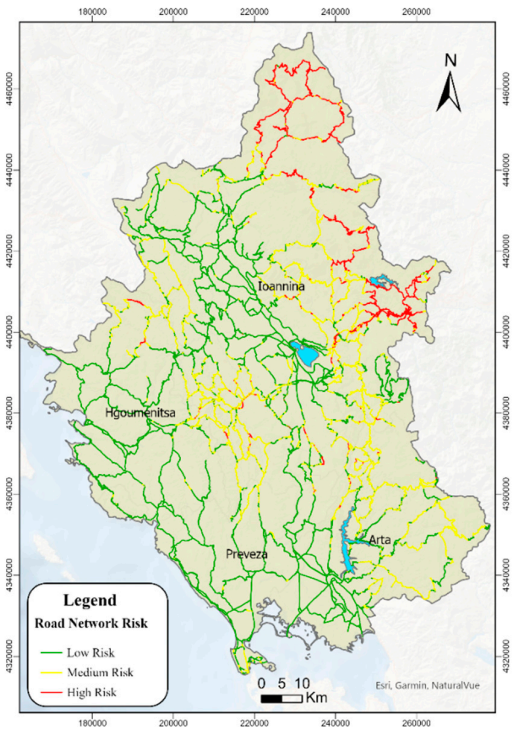

Figure 11. Landslide Risk Map of the Region of Epirus Road Network.

 doi:10.20944/preprints202604.1639.v1

5. Discussion

The quantitative framework implemented in this research highlights the critical importance of integrating multi-parametric environmental data to assess landslide risk of road infrastructure on a regional scale. By utilizing a detailed inventory of 295 field-verified active landslides, this study successfully identified the primary geo-environmental drivers of landslide occurrence in the Region of Epirus. The bivariate Frequency Ratio (FR) model served as a transparent and effective statistical tool, revealing that lithology and slope inclination are the most influential intrinsic factors. Specifically, flysch formations—which dominate the geological landscape of the Pindus mountain range—showed the highest susceptibility, with FR values reaching 2.39. This is scientifically consistent with the highly tectonized and sheared nature of flysch formations, which behave as weak, soil-like masses when weathered. Furthermore, the analysis of slope inclination confirmed an extreme correlation with instability on gradients exceeding 45°, where the FR value spiked to 4.43, indicating that topographical steepness is a fundamental precursor to failure in this rugged terrain.

A significant finding of this discussion is the role of cumulative annual precipitation as a landslide predisposing factor. The research utilized high-resolution ERA5-Land reanalysis data to overcome the limitations of sparse ground-based monitoring in mountainous areas. The statistical results identified that when areas receiving between 1,310 mm and 1,573 mm of annual rainfall FR exhibits the value of 2.03, suggesting that moderate-to-high precipitation levels initiating the occurrence of landslides. This underscores the necessity of including climatic variables in susceptibility modeling to capture the temporal-spatial reality of Mediterranean environments. By evaluating six different scenarios, Scenario n.1 was determined to be the optimal predictive model. This comprehensive configuration, which includes all five predisposing factors, successfully concentrated nearly 80% of the study area within the Moderate to Very High susceptibility zones, providing a more sensitive and precise risk identification than models that excluded key variables like rainfall or lithology.

Following the susceptibility assessment, the functional transformation of the Landslide Susceptibility Index (LSI) into a Landslide Hazard Index (LHI) was performed by adopting the methodological assumption of P=1. This transition was a strategic choice necessitated by the lack of multi-temporal historical frequency data. This approach ensures that the analysis remains proactive, focusing on areas with high geological predisposition as immediate sources of hazard. Consequently, it allowed the spatial distribution of susceptibility to serve as an operational tool for identifying segments of the road network directly exposed to landslide threats and enabled the integration with the road vulnerability.

The integration of the Landslide Hazard Index (LHI) with the weighted vulnerability of the road network provides a practical application of the statistical results for regional infrastructure management. The decision of this study to assign vulnerability weights based on traffic volume and functional importance (National, Provincial, and Local roads) ensures that the risk map reflects potential socio-economic disruption rather than just physical hazard. The final quantification of landslide risk was achieved by integrating hazard, road exposure and vulnerability components, by spatially multiplying these variables int a GIS environment, and classifying the road network into three distinct landslide risk levels: low, moderate and high.

The results indicate that the most critical risk zones are clustered along major transportation corridors that traverse flysch-dominated and steep mountainous sectors. While the lack of temporal frequency data necessitated the conservative assumption of a temporal probability equal to unity, the resulting Landslide Risk Map remains a vital operational tool. It allows regional authorities to move beyond reactive disaster management toward a proactive strategy of targeted geotechnical monitoring and prioritized infrastructure reinforcement.

6. Conclusions

This study has successfully established a geospatial framework for regional landslide risk assessment, specifically focused on protecting the 4,523 km road network of the Region of Epirus. Through the application of the Frequency Ratio model and the subsequent development of the

 doi:10.20944/preprints202604.1639.v1

Landslide Susceptibility Index (LSI), the research demonstrated that a holistic approach incorporating lithology, slope, elevation, land use, and precipitation is essential for accurate risk mapping. The selection of Scenario n.1, with all the pre-disposing factors, proved to be the most reliable model confirming that landslide phenomena in the Region of Epirus are driven by a complex synergy of geological weaknesses and steep terrain. The high predictive capability of this model, classifying the majority of the region into significant susceptibility zones, validates the use of bivariate statistical methods for large-scale regional planning.

The final product of this research, a comprehensive Landslide Risk Map, serves as a primary decision-support tool for local and regional governance. By identifying high-priority road segments where high hazard intersects with critical vulnerability, the map enables the strategic allocation of limited financial resources for slope stabilization and maintenance. Furthermore, the study emphasizes the critical value of regional landslide inventories, such as the He.L.P. platform, which provides the field-verified data necessary for robust statistical validation. As climate change is expected to increase the frequency of extreme rainfall events, the predictive capabilities established here will become increasingly vital for enhancing the resilience of critical infrastructure.

In conclusion, the methodology presented offers a replicable and transparent workflow for other landslide-prone Mediterranean regions. While the current model relies on the conservative assumption of a constant temporal probability, future research should focus on integrating real-time meteorological monitoring and historical frequency data to refine the temporal aspect of the hazard index. Nevertheless, the current findings provide a scientifically rigorous foundation for mitigating the socio-economic impacts of landslides and ensuring the safety and connectivity of the regional transportation network in the face of evolving natural threats.

Author Contributions: Conceptualization, N.D.; methodology, Z.M., A.A., N.D., P.I. and A.K.; validation, Z.M. and N.D.; formal analysis, Z.M., A.A. and P.I.; investigation, Z.M., A.A., N.D., P.I. and A.K.; resources, Z.M., A.A., N.D., P.I. and A.K.; data curation, Z.M. and N.D; writing—original draft preparation, Z.M. and, N.D.; writing—review and editing, Z.M. and N.D.; visualization, Z.M., A.A. and P.I. supervision, N.D. and A.K.; project administration N.D. and A.K.; funding acquisition, N.D. and A.K. All authors have read and agreed to the published version of the manuscript.

Funding: This research was supported by the project AIMS – Development and testing of a shared, AI-based predictive model for the coordinated use of big data and for a joint monitoring system of landslide risk in the Adriatic–Ionian region, which is funded under the Interreg VI-B IPA Adriatic-Ionian (ADRION) 2021-2027 Cooperation Programme (Grant Number: IPA-ADRION00414), co-financed by the European Union.

Data Availability Statement: Data is available from the authors upon request.

Acknowledgments: The basic equipment of the monitoring system used in Metsovo was funded by the Regional Operational Programme Epirus, Greece, 2014–2020. Parts of the equipment that were subsequently upgraded were funded by the project IPA-ADRION00414 – Development and testing of a shared, AI-based predictive model for the coordinated use of big data and for a joint monitoring system of landslide risk in the Adriatic–Ionian region.

Acknowledgments: The authors would like to express their gratitude to the Hellenic Ministry of Infrastructure and Transport (General Secretariat of Infrastructure, General Directorate of Transport Infrastructure, Directorate of Road Infrastructure - D13) for providing the geospatial data regarding the functional classification of the road network in the Region of Epirus.

Conflicts of Interest: The authors declare no conflicts of interest.

References

1. Guzzetti, F.; Carrara, A.; Cardinali, M.; Reichenbach, P. Landslide hazard evaluation: A review of current techniques and their application in a multi-scale study, Central Italy. *Geomorphology* **1999**, *31*, 181–216.
2. UNDRR (United Nations Office for Disaster Risk Reduction). *Global Assessment Report on Disaster Risk Reduction 2019*; United Nations: Geneva, Switzerland, 2019.

 doi:10.20944/preprints202604.1639.v1

3. Froude, M.J.; Petley, D.N. Global fatal landslide occurrence from 2004 to 2016. *Nat. Hazards Earth Syst. Sci.* **2018**, *18*, 2161–2181.
4. Petley, D.N. Global patterns of loss of life from landslides. *Geology Today* **2012**, *28*, 66–70.
5. Schuster, R.L.; Highland, L.M. Socioeconomic and environmental impacts of landslides in the Western Hemisphere. *U.S. Geol. Surv. Open-File Rep.* **2001**, 01–276.
6. Nadim, F.; Kjekstad, O.; Peduzzi, P.; Herold, C.; Jaedicke, C. Global landslide and avalanche hotspots. *Landslides* **2006**, *3*, 159–173.
7. Gariano, S.L.; Guzzetti, F. Landslides in a changing climate. *Earth-Sci. Rev.* **2016**, *162*, 227–252.
8. Crozier, M.J. Deciphering the effect of climate change on landslide activity: A review. *Geomorphology* **2010**, *124*, 260–267.
9. Sabatakakis, N.; Koukis, G.; Vassiliades, E.; Lainas, S. Landslide susceptibility zonation in Greece. *Nat. Hazards* **2013**, 65, 523–543; https://doi.org/10.1007/s11069-012-0391-y
10. Lainas, S.; Sabatakakis, N.; Koukis, G. Rainfall thresholds for possible landslide initiation in wildfire-affected areas of western Greece. *Bulletin of Engineering Geology and the Environment* **2016**, 75(3), 883-896; https://doi.org/10.1007/s10064-015-0762-5
11. Lainas, S.; Depountis N.; Sabatakakis, N. Preliminary Forecasting of Rainfall-Induced Shallow Landslides in the Wildfire Burned Areas of Western Greece. *Land* **2021**, 10(8):877; https://doi.org/10.3390/land10080877
12. Depountis, N.; Michalopoulou, M.; Kavoura, K.; Nikolakopoulos, K.; Sabatakakis, N. Estimating soil erosion rate changes in areas affected by wildfires. *ISPRS Int. J. Geo-Information* **2020**, *9*(10), 562; https://doi.org/10.3390/ijgi9100562
13. Boumpoulis, V.; Depountis, N.; Dimas, A.; Papatheodorou, G. Presentation and analysis of the Geotechnical Coastal Vulnerability Index and validation of its application to coastal erosion problems. *Sci. Rep.* **2025**, 15, 1424; https://doi.org/10.1038/s41598-025-85594-y
14. Depountis, N.; Sabatakakis, N.; Kavoura, K.; Nikolakopoulos, K.; Elias, P.; Drakatos, G. Establishment of an Integrated Landslide Early Warning and Monitoring System in Populated Areas. In Understanding and Reducing Landslide Disaster Risk; Casagli, N., Tofani, V., Sassa, K., Bobrowsky, P.T., Takara, K., Eds.; Springer: Cham, Switzerland, **2021,** pp. 263–274; https://doi.org/10.1007/978-3-030-60311-3_21
15. Guzzetti, F.; Peruccacci, S.; Rossi, M.; Stark, C.P. Rainfall thresholds for the initiation of landslides in central and southern Europe. *Meteorol Atmos Phys* **2007**, 98:239–267; https://doi.org/10.1007/s00703-007-0262-7
16. Segoni, S., Piciullo, L., Gariano, S.L. A review of the recent literature on rainfall thresholds for landslide occurrence. *Landslides* **2018**, 15:1483–1501; https://doi.org/10.1007/s10346-018-0966-4
17. Guzzetti, F.; Mondini, A.C.; Cardinali, M.; Fiorucci, F.; Santangelo, M.; Chang, K.T. Landslide inventory maps: New tools for an old problem. *Earth-Sci. Rev.* **2012**, 112, 42–66.
18. Reichenbach, P.; Rossi, M.; Malamud, B.D.; Mihir, M.; Guzzetti, F. A review of statistically-based landslide susceptibility models. *Earth-Sci. Rev.* **2018**, 180, 60–91.
19. Günther, A.; Reichenbach, P.; Malet, J.P.; van den Eeckhaut, M.; Hervás, J.; Dashwood, C.; Guzzetti, F. Tier-based approaches for landslide susceptibility assessment in Europe. *Landslides* **2014**, 11, 529–546.
20. Günther, A.; Van Den Eeckhaut, M.; Malet, J.-P.; Reichenbach, P.; Hervás, J. Climate-physiographically differentiated Pan-European landslide susceptibility assessment using spatial multi-criteria evaluation and transnational landslide information. *Geomorphology* **2014**, 224: 69-85; https://doi.org/10.1016/j.geomorph.2014.07.011
21. Wilde, M.; Günther, A.; Reichenbach, P.; Malet, J.P.; Hervás, J. Pan-European landslide susceptibility mapping: ELSUS Version 2. *Nat. Hazards Earth Syst. Sci.* **2018**, 18, 2929–2948.
22. Kirschbaum, D.B.; Stanley, T.; Zhou, Y. Spatial and temporal analysis of a global landslide catalog. *Nat. Hazards Earth Syst. Sci.* **2015**, *15*, 741–758.
23. Kirschbaum, D.B.; Stanley, T.; Zhou, Y. The Global Landslide Catalog (GLC): Overview and lessons learned. *Earth Syst. Sci. Data* **2019**, *11*, 1079–1092.
24. Fell, R.; Corominas, J.; Bonnard, C.; Cascini, L.; Leroi, E.; Savage, W.Z. Guidelines for landslide susceptibility, hazard and risk zoning for land use planning. *Engineering Geology* **2008**, 102: 85-98; https://doi.org/10.1016/j.enggeo.2008.03.022

 doi:10.20944/preprints202604.1639.v1

25. Hellenic Survey of Geology and Mineral Exploration (HSGME). National Landslide Inventory of Greece; Athens, Greece, 2025.
26. Laboratory of Engineering Geology, University of Patras. Hellenic Landslide Platform (He.L.P.): Web-Based GIS for Landslide Inventory and Monitoring; Patras, Greece, **2025**. Available online: https://patrasuni.maps.arcgis.com/apps/webappviewer/index.html?id=9ee309f77fca4790a64c716965c99e88 (accessed on 31 December 2025).
27. Guzzetti, F.; Reichenbach, P.; Cardinali, M.; Galli, M.; Ardizzone, F. Probabilistic landslide hazard assessment at the basin scale. Geomorphology **2005**, 72, 272–299. https://doi.org/10.1016/j.geomorph.2005.06.002
28. Kavoura, K.; Sabatakakis, N. Investigating landslide susceptibility procedures in Greece. Landslides **2020**, 17, 127–145. https://doi.org/10.1007/s10346-019-01271-y
29. UNISDR. Living with Risk: A Global Review of Disaster Reduction Initiatives; United Nations International Strategy for Disaster Reduction: Geneva, Switzerland, **2004**.
30. Corominas, J.; van Westen, C.; Frattini, P.; Cascini, L.; Malet, J.P.; Fotopoulou, S.; et al. Recommendations for the quantitative analysis of landslide risk. Bull. Eng. Geol. Environ. **2014**, 73, 209–263. https://doi.org/10.1007/s10064-013-0538-8
31. Fell, R.; Ho, K.K.S.; Lacasse, S.; Leroi, E. A framework for landslide risk management. In Landslide Risk Management; Hungr, O., Fell, R., Couture, R., Eberhardt, E., Eds.; Taylor & Francis: London, UK, **2005**, pp. 3–25.
32. Lee, S.; Talib, A.T. Probabilistic landslide susceptibility and factor effect analysis. Environ. Geol. **2005**, 47, 982–990. https://doi.org/10.1007/s00254-005-1228-z.
33. Lee, S.; Pradhan, B. Landslide hazard mapping at Selangor, Malaysia using frequency ratio and logistic regression models. Landslides **2007**, 4, 33–41. https://doi.org/10.1007/s10346-006-0047-y.
34. Ferentinou, M.; Chalkias, C. Mapping Mass Movement Susceptibility Across Greece with GIS, ANN and Statistical Methods. In Landslide Science and Practice; Margottini, C., Canuti, P., Sassa, K., Eds.; Springer: Berlin/Heidelberg, Germany, **2013**, pp. 209–216.
35. Papanikolaou, D.I. The Geology of Greece; Springer: Cham, Switzerland, **2021**. ISBN: 978-3-030-60730-2.
36. Cruden, D.M.; Varnes, D.J. Landslide Types and Processes. In Landslides: Investigation and Mitigation; Turner, A.K., Schuster, R.L., Eds.; Transportation Research Board, Special Report 247; National Academy Press: Washington, DC, USA, **1996**, pp. 36–72.
37. Hungr, O.; Leroueil, S.; Picarelli, L. The Varnes classification of landslide types, an update. Landslides **2014**, 11, 167–194. https://doi.org/10.1007/s10346-013-0436-y
38. CORINE Land Cover. CLC2018. European Union, Copernicus Land Monitoring Service (CLMS) **2018**. Available online: https://land.copernicus.eu/en/products/corine-land-cover/clc2018 (accessed on 31 December 2025).
39. Muñoz Sabater, J. ERA5-Land hourly data from 1950 to present; Copernicus Climate Change Service (C3S) Climate Data Store (CDS), **2019**. https://doi.org/10.24381/cds.e2161bac (accessed on 31 December 2025).
40. Hersbach, H.; Bell, B.; Berrisford, P.; Hirahara, S.; Horányi, A.; Muñoz-Sabater, J.; et al. The ERA5 global reanalysis. Q. J. R. Meteorol. Soc. **2020**, 146, 1999–2049. https://doi.org/10.1002/qj.3803
41. Shepard, D. A Two-Dimensional Interpolation Function for Irregularly-Spaced Data. In Proceedings of the 1968 23rd ACM National Conference; ACM: New York, NY, USA, **1968**; pp. 517–524.
42. Evans, I.S. The Selection of Class Intervals in Cartography. The Cartographic Journal **1977**, 14, 98–124. https://doi.org/10.1179/caj.1977.14.2.98
43. Hellenic National Meteorological Service (HNMS). Technical Guidance on Hypsometric Classification for Civil Protection; Document No. Φ.970/ΑΔ:7753/Σ1863; HNMS: Athens, Greece, **2012**.
44. Jenks, G.F. The Data Model Concept in Statistical Mapping. Int. Yearb. Cartogr. **1967**, 7, 186–190.